UCRL-ID-123147

A Final Report to the Laboratory Directed Research and Development Committee on Project 93-ERP-075: "X-ray Laser Propagation and Coherence: Diagnosing Fast-evolving, High-density Laser Plasmas Using X-ray Lasers"

A. S. Wan, R. Cauble, L. B. Da Silva, S. B. Libby, J. C. Moreno

February 1996

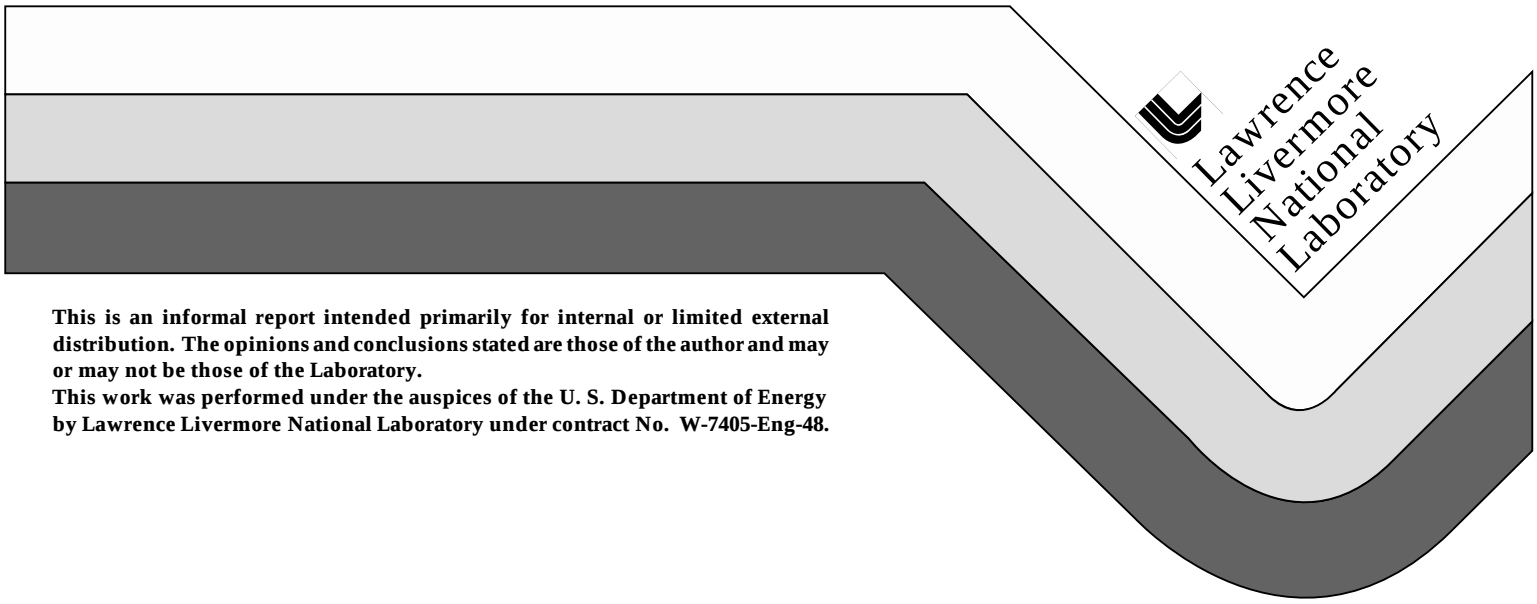

This work was performed under the auspices of the U. S. Department of Energy by Lawrence Livermore National Laboratory under contract No. W-7405-Eng-48.

A Final Report to the Laboratory Directed Research and Development Committee on Project 93-ERP-075: "X-ray Laser Propagation and Coherence: Diagnosing Fast-evolving, High-density Laser Plasmas Using X-ray Lasers"

Principle Investigator
Alan S. Wan

Co-investigators
Robert Cauble, Luiz B. Da Silva, Stephen B. Libby, Juan C. Moreno

Lawrence Livermore National Laboratory
Livermore, CA 94550, U. S. A.

Abstract

This report summarizes the major accomplishments of this three-year Laboratory Directed Research and Development (LDRD) Exploratory Research Project (ERP) entitled "X-ray Laser Propagation and Coherence: Diagnosing Fast-evolving, High-density Laser Plasmas Using X-ray Lasers," tracking code 93-ERP-075 The most significant accomplishment of this project is the demonstration of a new laser plasma diagnostic: a soft x-ray Mach-Zehnder interferometer using a neonlike yttrium x-ray laser at 155 Å as the probe source. Detailed comparisons of absolute two-dimensional electron density profiles obtained from soft x-ray laser interferograms and profiles obtained from radiation hydrodynamics codes, such as LASNEX, will allow us to validate and benchmark complex numerical models used to study the physics of laser-plasma interactions. Thus the development of soft x-ray interferometry technique provides a mechanism to probe the deficiencies of our numerical models and is an important tool for the high-energy density physics and science-based stockpile stewardship programs. We have used the soft x-ray interferometer to study a number of high-density, fast evolving, laser-produced plasmas, such as the dynamics of exploding foils and colliding plasmas. We are pursuing the application of the soft x-ray interferometer to study ICF-relevant plasmas, such as capsules and hohlraums, on the Nova 10-beam facility. We have also studied the development of enhanced-coherence, shorter-pulse-duration, and high-brightness x-ray lasers. The utilization of improved x-ray laser sources can ultimately enable us to obtain three-dimensional holographic images of laser-produced plasmas.

1. Introduction

Since the first demonstration of a soft x-ray laser at the Lawrence Livermore National Laboratory (LLNL), [1] x-ray lasers have been considered for applications in the fields of microscopy, holography, material science, and plasma physics. [2] With its short wavelength (40–400 Å), short controllable pulse duration, high peak brightness, and sufficient spatial and temporal coherence, x-ray laser is ideally suited as a plasma diagnostic to image rapidly evolving (< 1 ns) laser-driven plasmas with high electron densities (10^{21} cm^{-3} < n_e < 10^{24} cm^{-3}).

Beginning from Fiscal Year (FY) 1993, we carried out a Laboratory Directed Research and Development (LDRD) project, entitled "X-ray Laser Propagation and Coherence: Diagnosing Fast-evolving, High-density Laser Plasmas Using X-ray Lasers." This project is funded by the Exploratory Research Program (ERP) of Defense Science Department, to study the development and application of laser plasma diagnostics using x-ray lasers. We benefited from recent advances in the development of short wavelength multilayer mirrors and beamsplitters in the soft x-ray regime, [3] which enabled us to make the leap forward in utilizing x-ray lasers to probe laser plasmas with parameters that were previously inaccessible using conventional optical instruments.

This LDRD project was successfully completed in FY1995, delivering a new diagnostic, a soft x-ray interferometer, to measure two-dimensional (2-D) density profiles of large-scale-length, fast-evolving, high-density laser produced plasmas. We used a Nova-driven, collisionally pumped neonlike yttrium soft x-ray laser, operating at 155 Å, as the source of our soft x-ray interferometer. Detailed comparisons of absolute 2-D electron density profiles obtained from soft x-ray laser interferograms and profiles obtained from radiation hydrodynamics codes, such as LASNEX, will allow us to validate and benchmark complex numerical models used to study the physics of laser-plasma interactions. Thus the development of soft x-ray interferometry technique provides a mechanism to probe the deficiencies of our numerical models and is an important tool for the high-energy-density physics and science-based stockpile stewardship programs. Prior to the demonstration of the soft x-ray interferometer, we used x-ray lasers as high fluency monochromatic radiographic sources, radiographic images of smooth-laser accelerated foils have shown small-scale (~10 μm) filamentation which may reveal limitations to direct-drive inertial confinement fusion (ICF) capsules due to unexpectedly intense hydrodynamic instabilities. [4] We have also used x-ray lasers to measure one-dimensional (1-D) density gradients of laser plasmas using the Moiré deflectometry technique. [5]

The impact of this project is widely recognized in international physics communities, resulting in a number of invited presentations at international physics conferences and many journal and conference papers. This paper is a brief summary of the technical achievements of this LDRD-funded project. For more detail the readers are directed to the conference and journal publications that resulted from this LDRD-funded project which is listed in the Appendix. In Sec. 2 of this paper we describe the soft x-ray laser interferometer. We present some examples of how we can apply this new innovative instrument to study plasmas that are relevant to high-energy-density physics in Sec. 3. We have also invested resource to develop enhanced coherence x-ray lasers and we summarize our results in Sec. 4. Section 5 describes some of the future applications of this instrument for both commercial applications and basic physics research. We summarize in Sec. 6.

2. The Development of Soft X-ray Interferometer

2.1 Accessibility Regime

To obtain accurate and absolute measurements of electron density profiles for high density, laser-produced plasmas, optical interferometry has been used to study exploding foils for x-ray laser dynamics, [6,7,8] to examine profile steepening due to radiation pressure, [9] and to study filamentation instabilities. [10,11] However, the size and density regimes of the laser plasma accessible to an optical interferometer are limited by inverse bremsstrahlung absorption and refractive propagation of probe beams facing large density gradients. By employing a shorter wavelength x-ray laser, as compared to using conventional optical lasers as the probe source, we can access a much higher density regime while reducing refractive effects which limit the spatial resolution and data interpretation.

In a plasma, the index of refraction, n_{ref}, is related to the critical electron density, $n_{cr} = 1.1\times10^{21}\ \lambda^{-2}$ [cm^{-3}] (λ is the wavelength of the probe laser in μm), by $n_{ref} = \sqrt{1 - n_e/n_{cr}}$. In an interferometer the number of fringe shifts, N_{Fringe}, is then given by

$$N_{Fringe} = \frac{\delta\phi}{2\pi} = \frac{1}{\lambda}\int_0^L (1 - n_{ref})\, dl \approx \frac{n_e}{2n_{cr}}\frac{L}{\lambda}, \qquad (1)$$

where L [μm] is the path length across the target plasma and we assume refraction effects are negligible. Experimentally the maximum number of fringe shifts measurable is usually constrained by detector resolution and is rarely greater than ~50. This imposes a constraint on the product $n_e L$ for a given wavelength.

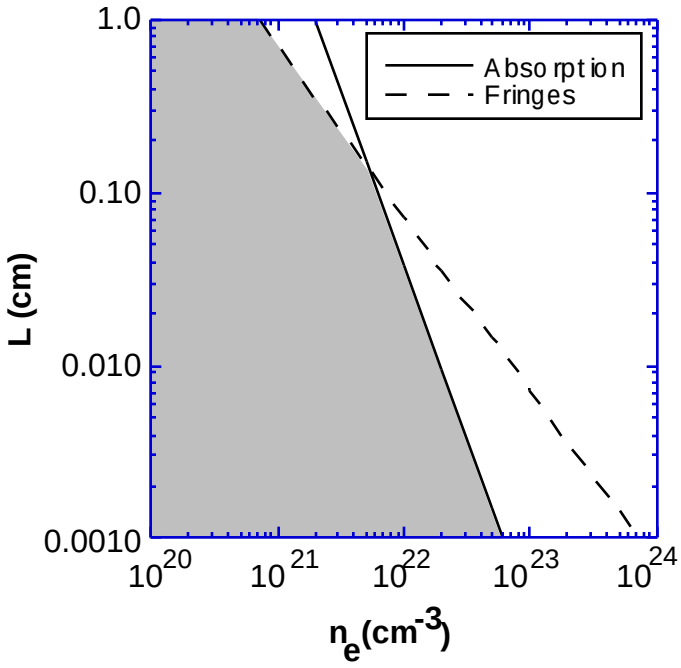

Figure 1. The shaded portion represents the regime of electron density and plasma dimension accessible with a soft x-ray laser source (155 Å) which is constrained by free-free absorption and a maximum of 50 fringe shifts.

An additional constraint which limits the accessible density and length parameter space is absorption. In a plasma dominated by free-free absorption the absorption coefficient, α (in units of cm^{-1}), is approximately given by [12]

$$\alpha \approx 2.44 \times 10^{-37} \frac{\langle Z^2 \rangle n_e n_i}{\sqrt{kT}\,(h\nu)^3}\left[1 - \exp\left(\frac{-h\nu}{kT}\right)\right], \qquad (2)$$

where the electron temperature, kT, and photon energy, $h\nu$, are in eV and electron and ion densities are in cm^{-3}. The strong scaling with photon energy shows the advantage of probing with soft x-ray sources. For most high temperature plasmas of interest, the level of ionization is sufficient to eliminate any bound-free absorption in the soft x-ray region. Resonant line absorption is possible but very unlikely given the narrow bandwidth of the x-ray laser, ~0.01 Å. [13] Therefore, if we consider only free-free absorption in a plasma with 1 keV temperature and average ionization of 30 (mid-Z plasma) we obtain from Eqn. 2, $\alpha \approx 2.6\text{x}10^{-43} n_e^2$. If we allow for one optical depth (i.e. $\alpha L = 1$) of absorption we obtain $n_e^2 L = 3.8\text{x}10^{42}$. In Figure 1 the shaded region represents the electron density and plasma dimension accessible with a soft x-ray laser source (155 Å) which is constrained by free-free absorption and a maximum of 50 fringe shifts. This parameter space easily covers plasmas normally produced in the laboratory.

2.2 Instrumentation

Extending conventional interferometric techniques into the soft x-ray range has been difficult because of the problems with designing optical systems which operate in the range 40-400 Å. Fortunately, multilayer mirror technology has now evolved to the point where artificial structures can be routinely fabricated with reflectivities as high as 65% at 130 Å, [14,15] and with the overall uniformities required by more conventional interferometers. We have also successfully fabricated high quality, large active area (1.2 cm x 1.2 cm) beamsplitters with excellent reflectivity and transmission at short wavelengths. Utilizing these multilayer optical components and a collisionally pumped neon-like yttrium x-ray laser operating at 155 Å as the probe source, we have successfully demonstrated a soft x-ray laser interferometer in a skewed Mach-Zehnder configuration.

The experimental setup used to probe plasmas is shown schematically in Figure 2. The system consists of a collimated x-ray laser source, an imaging mirror and a skewed Mach-Zehnder interferometer. In order to reduce background self-emission, a series of three multilayer mirrors were used prior to the CCD detector, reducing the bandpass of the system. The effective bandpass of this system was 0.4 nm, which is significantly broader than the 0.01 Å spectral width of the x-ray laser source. The image magnification was 19 giving a pixel limited resolution of ~1.3 μm. Reference 16 gives a detailed description of the instrumentation.

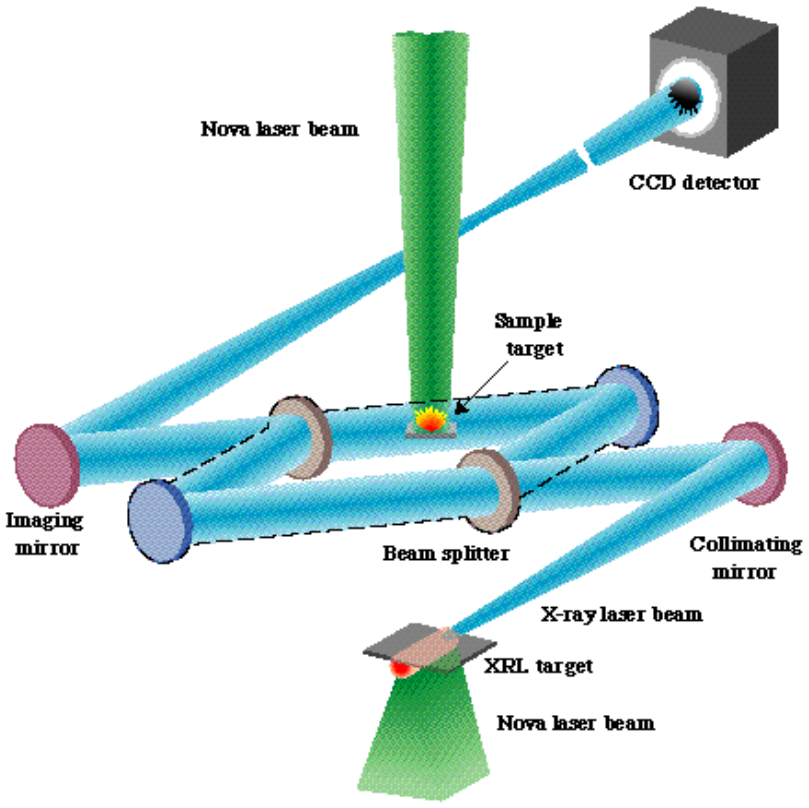

Figure 2. Experimental setup of the soft x-ray laser interferometer system which consists of a collimated x-ray laser source (formed at the bottom with the collimating mirror), an interferometer in a skewed Mach-Zehnder configuration (shown with dashed outline) with the sample target irradiated by another Nova laser beam (coming from the top), and an imaging mirror.

The transmissive and reflective properties of the multilayer components, at the appropriate wavelength and operating angles, were characterized prior to the experiment. The multilayer mirrors have a peak reflectivity of 60±5% at 155 Å. The beamsplitters used in the interferometer are the most critical element of the system. The measured reflectivity and transmission for these beamsplitters at 155 Å were 20% and 15% respectively. The overall throughput of each arm, accounting for the mirror and beamsplitter (one transmission & one reflection), was ~ 0.6 x 0.20 x 0.15 = 18%.

A collisionally pumped neon-like yttrium x-ray laser operating at 155 Å was used as the probe source. The x-ray laser was produced by irradiating a solid 3-cm-long yttrium target with one beam from Nova (0.53 μm, 600-ps-long square pulse) at an intensity of 1.5×10^{14} W/cm^2. The x-ray laser has an output energy of 3±2 mJ, a FWHM divergence of ~10-15 mrad and an output pulse width of 350 ps. The short pulse and high brightness of the x-ray laser allowed us to obtain an interferogram in a single 350 ps exposure thereby reducing the effects of vibrations and motion blurring. The timing between the two Nova lasers, one to generate the x-ray laser and one to produce the target plasma, was defined by the time-of-flight path of our interferometer setup and the desired probe time. Reference 17 describes the measurement of the transverse and temporal coherence properties of the x-ray laser which are important in the design of our interferometer.

3. Application of Soft X-ray Interferometer

We have performed a variety of experiments in the demonstration of the soft x-ray laser interferometer. We have measured electron densities exceeding 2×10^{21} cm^{-3} in a CH plasma which is millimeters in extent. [18] In the analysis of the CH experiment we described the effect of three-dimensional (3-D) hydrodynamic expansion of laser-produced plasmas on the data interpretation and analysis. We have also measured of the density profile of a selenium and yttrium exploding foil commonly used for x-ray laser targets. [19] In using a yttrium x-ray laser to image a thin yttrium exploding foil, we measured small signal gain of order 20 cm-1, validating the prediction of atomic physics calculations and confirming the impact of refraction on the output of x-ray lasers which resulted in low measured gain. Most recently we have began using the interferometer to study plasma interpenetration and stagnation in a colliding plasma configuration. [20] In this report we briefly describe our experiments on the selenium exploding foil and colliding plasmas as examples of the applications of soft x-ray interferometry.

We typically use LASNEX [21] in an axisymmetric two-dimensional (2-D) configuration for our data analysis. LASNEX includes many physics models necessary to simulate a multi-dimensional radiative hydrodynamics problem, including laser-matter interaction, radiation transfer, electron thermal diffusion by conduction, and simple description of non-local thermodynamic equilibrium atomic kinetics. Reference 21 includes a description of the physics models used in LASNEX. The LASNEX parameters used are based on simulations that yielded the best agreements between simulations and past experiments. These parameters may vary depending on the physical regime of the problem. For example, in LASNEX, we employ a flux-limited thermal diffusion model for the electron energy transport. The value of the flux limiter determines the degree of the artificial reduction of the thermal flux. Past studies [22,23,24,25,26] have found that by varying the flux limiter, which can range from strongly flux-limited diffusion to no reduction, better agreements between simulated and measured profiles of temperatures, densities, and x-ray conversion can be achieved. It is the validity and benchmarking of these numerical models, with the absolute n_e measurements at high densities, that are the primary reasons for performing experiments using soft x-ray interferometry.

3.1 Density Profiles of Selenium Exploding Foils

To reduce the effect of refraction and to attain high gain in a laser-driven configuration, the exploding-foil technique was designed and employed for achieving the first soft x-ray laser in neon-like selenium [27,1] Experiments [22,27,28] were performed to test the modeling of the exploding foil and found good agreements between the simulation and n_e profile inferred from

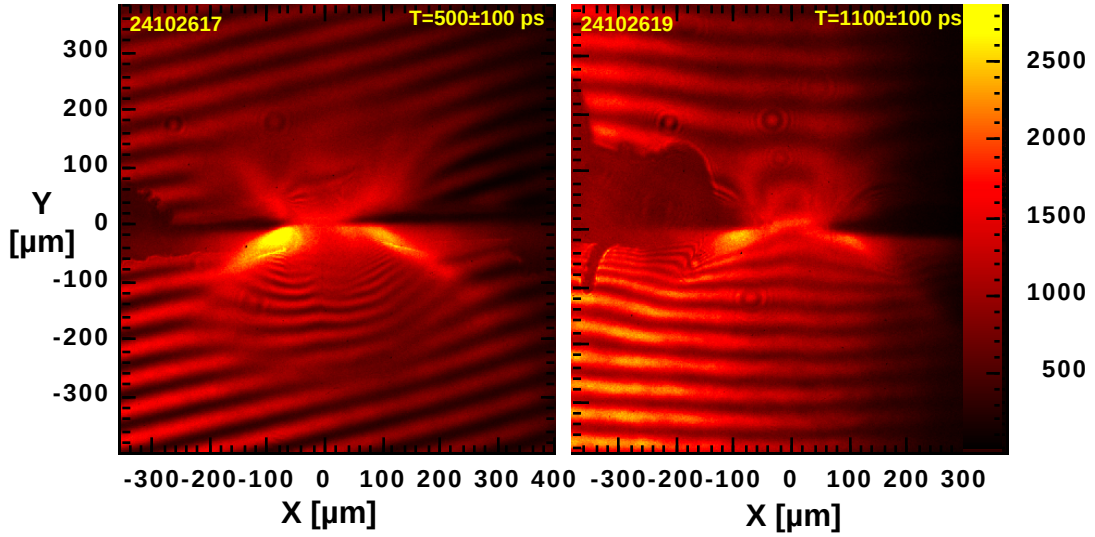

Figure 3 Interferograms of exploding selenium foil at two different times taken at 155 Å. The scale on the right hand side indicates the intensity level of the exposure.

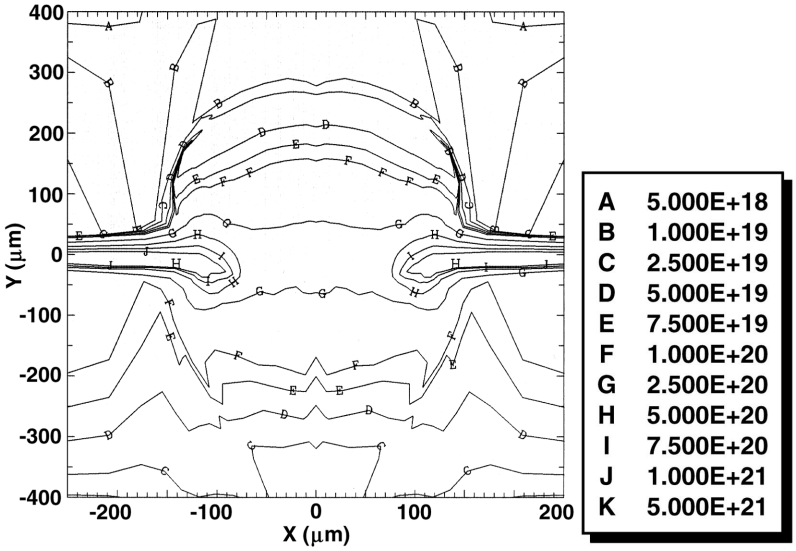

Figure 4. Snap shot of the 2-D electron density profile at 500 ps into the laser pulse.

Abel inversion of the interferogram. A 0.26-mm probing laser of 20 ns duration was used as the probing source that produced the interferograms. [29] We have repeated the selenium exploding foil experiment using the soft x-ray laser interferometry technique. The shorter wavelength of the yttrium x-ray laser and our optical setup allow us to probe a large area plasma at much higher density and with much better spatial resolution.

In Fig. 3 we show two interferograms showing the plasma evolution in an exploding selenium foil experiment. A 600-ps-long, temporally squared, line focused optical laser incident from the bottom on a 200-nm thick, 1-mm wide (in the *z*-direction along the x-ray laser probe beam) selenium foil heats and expands the plasma to produce a large hot plasma. The left interferogram is

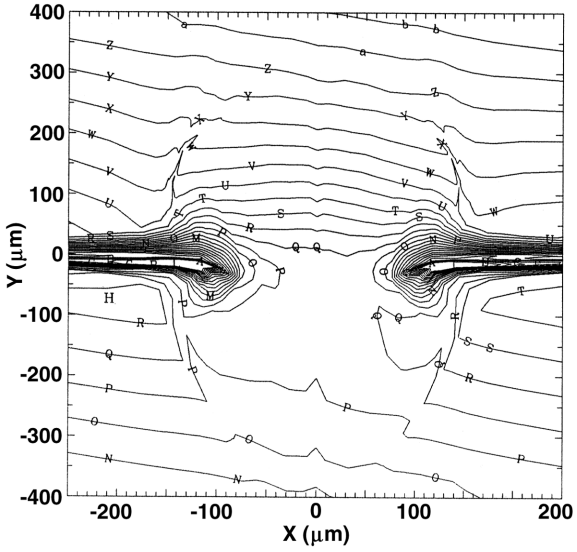

Figure 5. Reconstructed interferogram using the n_e profile shown in Fig. 4, assuming a fixed plasma length of 1 mm and neglecting the effect of refraction and hydrodynamic expansion along the line focus

taken at near the end of the 600-ps drive pulse (500 ± 100 ps) while the right interferogram was taken at a time (1100 ± 100 ps) long after the end of the driving laser pulse. The fast plasma expansion and subsequent laser burn through is clearly observed.

The double-humped structure of the 500 ps interferogram is likely due to the imprinting of non-gaussian spatial distribution of the laser line focus in the *y*-direction. Two-dimensional simulations indicate that we can duplicate the double-humped structure by imposing a 5% intensity depression at the center of the line focus. Such deviation from a perfectly gaussian-shaped spatial distribution is possible since experimentally we achieve the best focus using visual alignment.

Figure 4 is a plot of a snap shot of the LASNEX-calculated 2-D n_e profile at 500 ps into the pulse, at a time within the exposure window for the interferogram shown on the left hand side of Fig. 3. From the 2-D n_e profile we can construct a simulated interferogram, shown in Fig. 5, to compare with the measured interferogram, assuming a plasma length of 1 mm and neglecting the effect of refraction and hydrodynamic expansion along the line focus. We obtained very good agreement between the simulated and measured interferograms.

Taking a cut along the center of the line focus, at $x = 0$, we compare in Fig. 6 the measured n_e profile with profiles obtained from LASNEX simulations at times of 400, 500, and 600 ps into the pulse. The experimental uncertainty is approximately 0.1 fringe, or ~ 1.4 x 10^{19} cm^{-3} (with 1-mm path length). Consider the various assumptions that went into the calculations, on the physics of

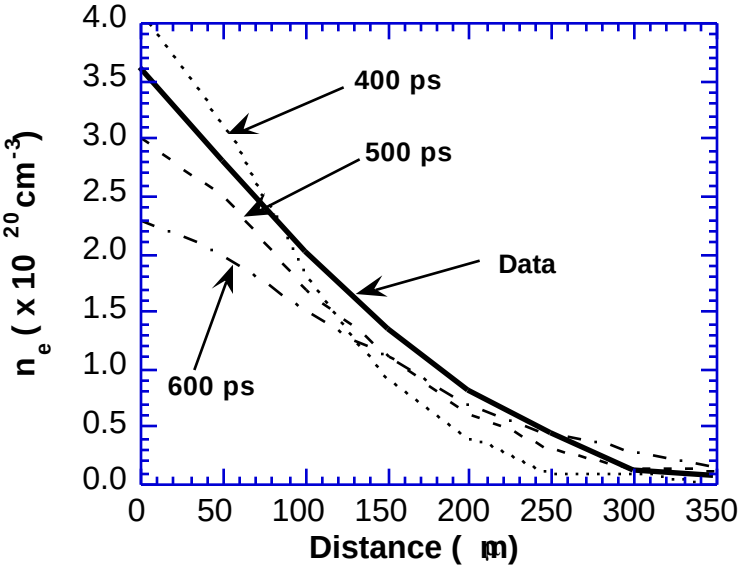

Figure 6. Comparisons between the measured n_e profiles at the center of the line focus ($x = 0$) and profiles obtained from LASNEX simulations at times of 400, 500, and 600 ps into the pulse.

laser energy deposition via inverse bremsstrahlung and resonance absorption, hydrodynamics, and heat conduction, the agreement is excellent.

4.2 Interpenetrating and Colliding Plasmas

The understanding of the collision and subsequent interaction of counter-streaming high-density plasmas is important for the design of indirectly-driven inertial confinement fusion (ICF) hohlraums [30] and x-ray lasers [31,32,33]. In a typical indirectly-driven ICF hohlraum, the interaction of the optical laser drive with high-Z (typically gold) inner hohlraum surfaces generates high-density plasma blowoff from the inner surface. In a vacuum hohlraum, these counterstreaming plasmas flow unimpeded and collide on the axis of cylindrically-shaped hohlraums. Single-fluid radiation hydrodynamics codes that we typically use to design ICF and other laser-plasma experiments, such as LASNEX, do not allow for plasma interpenetration. Without interpenetration, as the plasmas collide and stagnate, their kinetic energy converts to internal energy, resulting in unphysically large ion temperature which generates strong shocks. Furthermore, as the plasma stagnate on the hohlraum axis, the single-fluid codes predict the creation of jets of high-velocity and high-density plasmas, which stream toward the capsule located at the center of the hohlraum and destroy the symmetry of the capsule implosion before capsule ignition. Current hohlraum designs for Nova [34,35,36] and the point design for the National Ignition Facility (NIF) [30,36,37] employ a low-density fill gas to impede the plasma blowoff from stagnating on the hohlraum axis before the capsule ignition.

Past experimental studies of colliding plasmas have primarily focused on laser-produced, low-Z (aluminum, silicon, magnesium) front-illuminated thick targets [38,39,40,41,42,43] and back-illuminated exploding thin foils [44,45]. Most of the experiments utilizes x-ray spectroscopy and imaging techniques to characterize the plasma parameters, such as the measurement of electron temperature (T_e) through line-ratio and ionization balance, ion temperature (T_i) using line shape, and spatial and temporal images of the plasma collision using x-ray pinhole imaging. Chenais-Popovics et al. [44] also uses line ratios to estimate the electron density (n_e) profiles. Bosch et al. [38] employed a holographic interferometer at 2630 Å to measure snapshots of the n_e profiles.

The setup of our first colliding plasma experiment is shown in Figure 7. Two gold slabs are aligned at 45 deg with respect to the axis of symmetry. The minimum gap between the tips of the two slabs is 500 μm in this experiment. We generate a 500 μm full-width (FW) line-focused laser beam which incidents the slabs, as shown in Fig. 7(a), and generates plasmas blowing toward each other. The laser has an intensity on target of 3×10^{14} W/cm^2 and has a 1-ns squared temporal

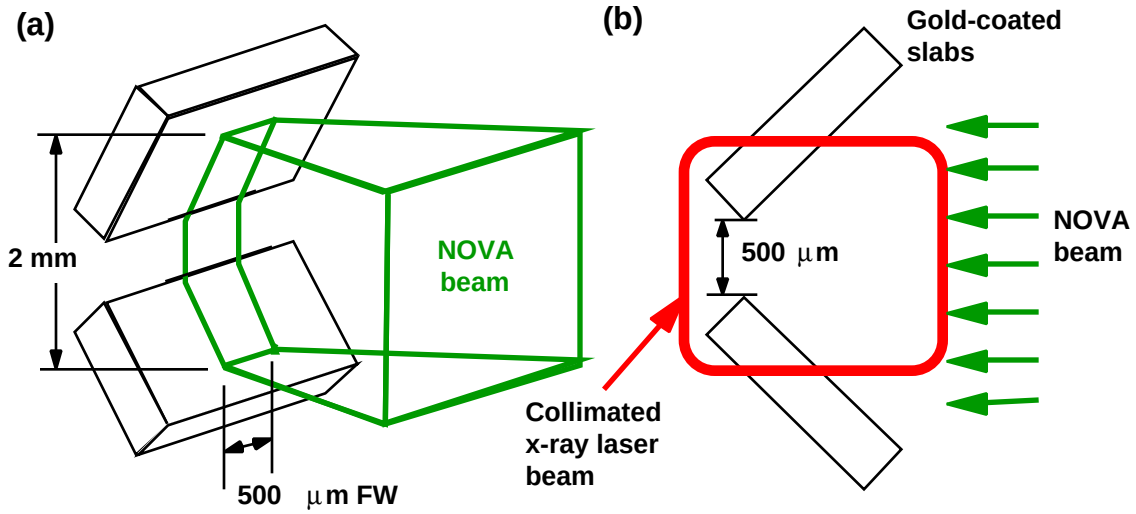

Figure 7. Experimental configuration for the colliding plasma experiment. (a) 3-D view of the Nova beam illuminating the 2 gold slabs oriented at 45 degrees with respect to the axis of symmetry. (b) side view showing the window of collimated x-ray laser beam which defines the view of the CCD camera.

pulse shape. At late time the two plasma streams collide at the axis of symmetry. By varying the geometry, the slab materials, and the intensity of the incident optical laser, we can change the collisionality of the plasma. At high density and low temperatures, the plasma behaves like a fluid where codes like LASNEX should be able to model accurately. The plasma shifts into a collisionless region with increasing temperature and reducing density, where we expect to observe significant plasma interpenetration.

The target was backlit edge-on by the x-ray laser beam 1 ns after the start of the laser pulse that generated the gold plasma. The side view of Fig. 7 shows the view in the direction of the collimated x-ray laser probe beam which was several millimeters in extend. In Fig. 8 we show the measured interferogram of the colliding plasma, in the geometry defined by the side view of Fig. 7(b). The image shows excellent fringe visibility. We also observed significant self emission from the plasma near the slab surface. We can further reduce the self emission in the future, improving the optical quality of the system by reducing the bandpass near the x-ray laser wavelength and by better temporal gating of our detector.

Near the symmetry axis between the two gold slabs we can clearly observe significantly greater fringe shifts as the results of the plasma collision. At the extreme left and right of the interferogram shown in Fig. 8 we can still see the unperturbed fringe pattern where there is no plasma. We can use these unperturbed fringes to reconstruct a unperturbed 2-D fringe mapping for the entire

coverage. We can then use that reconstructed mapping as a reference to measure the amount of fringe shift at any position due to the presence of the plasma. The beamsplitters were not perfectly flat, creating some minor variations in the unperturbed fringe pattern and that is one of our dominant experimental uncertainties. Based on previous null shots with similar quality beamsplitters, we estimate the uncertainty to be of order 0.1 fringe. We also assume a uniform plasma with a 500 μm path length, which is the transverse width of the optical laser line focus onto the gold slabs.

Figure 9 shows the measured 2-D n_e profile in the colliding geometry. The solid line in Fig. 10 represents a 1-D cut of the n_e profile at the x = 850 μm position of Fig. 9, approximately 250 μm from the tips of the slanted slabs. In the collisionless regime where the plasma is hot and at low density, n_e will just be the superpositioned density profiles from the two interpenetrating counterstreaming plasmas. The dotted line in Fig. 10 represents the n_e profile of two interpenetrating collisionless plasma streams. Here we observed significant density increase on-axis due to the collision with the measured n_e as high as 6 x 10^{20} cm^{-3}, which is a factor of 3-4 higher than the estimated n_e value without collision. The observed stagnation region has a width of order 100 μm. The plasma blowoff is in the direction normal to the slab surface. If we project a normal line from the slab edge, we can clearly observe density increase beyond the region where two counterstreaming plasmas collide, which indicate jetting of the stagnant plasma. It is this type of plasma jets which can distort the symmetry of the capsule.

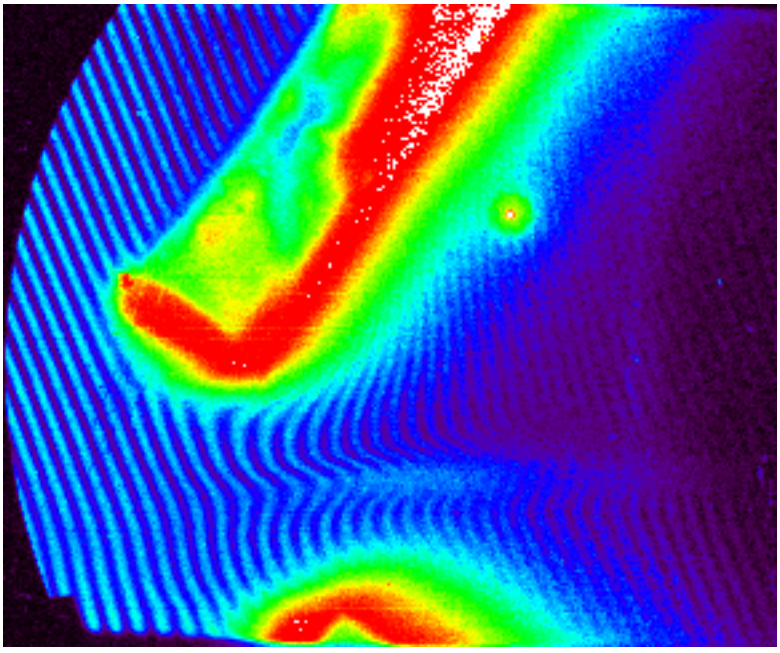

Figure 8 Measured interferogram of the colliding plasma. We observed excellent fringe visibility with strong self emission near the slab surface. Large fringe shifts on-axis is evident due to stagnation of the plasma in the colliding geometry. Null fringes are visible to the left of the slabs.

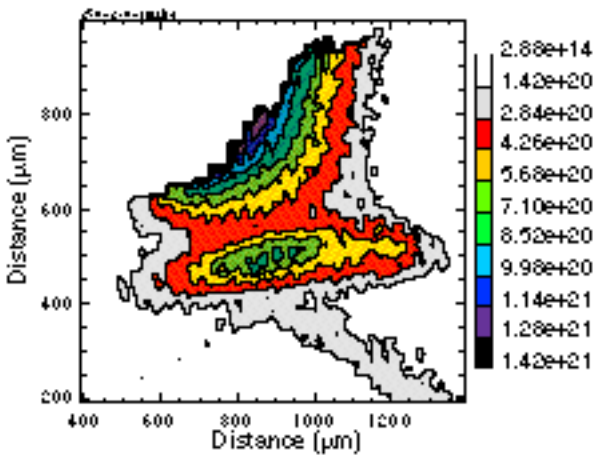

Figure 9 Measured 2-D n_e profile, assuming a uniform plasma with path length of 500 μm. At the symmetry axis we observed significant density increase due to plasma stagnation. n_e value on-axis is as high as 6 x 10^{20} cm^{-3}, which is a factor of 3-4 higher than the estimated n_e value without collision.

A strong motivation to perform the colliding plasma experiment is to examine the validity of LASNEX, which is a Lagrangian fluid code, in a regime that might deviate from the fluid behavior. Figure 11 shows a snapshot of a LASNEX-calculated 2-D n_e profile at a time of 150 ps after the end of a 1-ns-long, temporally squared optical laser pulse, which corresponds to the peak of the x-ray laser pulse that serves as the gate for our imaging setup used in the experiment. In this calculation we use a multi-group radiation diffusion method to account for the radiative effect. Neglecting the radiation opacity results in significantly lower plasma temperatures. In the blowoff plasma, T_e is as high as 3 keV. Using the three temperature (T_e, T_i, and T_r, the radiation temperature) approximation where the radiation is assumed to be optically thin, LASNEX predicts a T_e of order 0.5 keV. The change in the plasma parameters significantly impact the ionization balance and collisionality of the plasma.

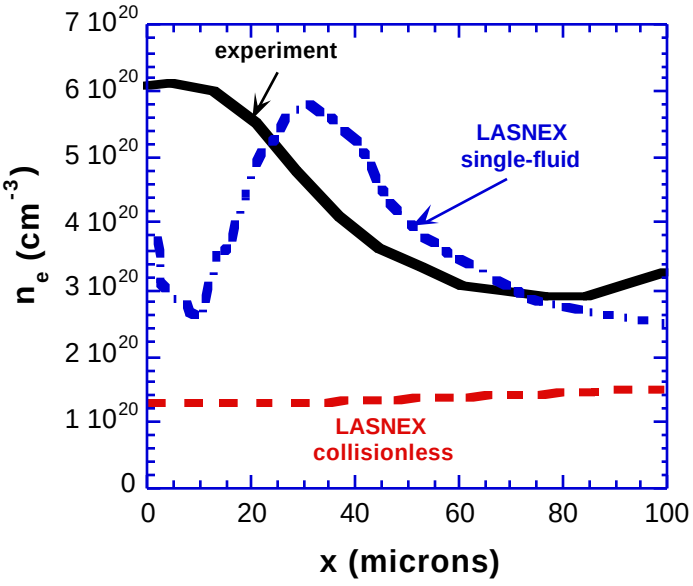

Figure 10 1-D cuts comparing experiment (solid line) with 2 LASNEX calculations using single-fluid, or fully collisional, (dash-dotted line) and collisionless (dashed line) approximations.

In Fig. 11 the symmetry axis at the top of the 2-D plot serves as a mirror reflectivity boundary condition. This geometry simulates the lower half slab of the experimental configuration shown in Fig. 7 with the optical Nova laser incident the thick gold slab from the right side. As the blowoff plasma reaches the symmetry axis, the velocity of the zone boundary for a Lagrangian code is set equal to zero, and the slowing and stagnation of the counterstreaming single-fluid plasmas results in the conversion of kinetic to internal energy. In this case T_i can reach a unphysically large values exceeding 10^3 keV. The resulting shock waves, whose intensity depends on the collisionality of the plasma, propagate away from the symmetry axis. The dash-dotted line of Fig. 10 is a 1-D cut of the 2-D n_e profile shown in Fig. 11, and at a corresponding position to the 1-D cut from the measured n_e profile, 250 μm from the slab tip. Although LASNEX predicts a comparable stagnation width of order 100 μm, the n_e profile peaks at ~ 30 μm off the symmetry axis and is very characteristic of the shock heated expansion predicted by LASNEX. The measured n_e profile falls inbetween the two calculated n_e profiles, representing the extremes of plasma collisionality. This set of comparison between experiment and calculations clearly shows the need for different

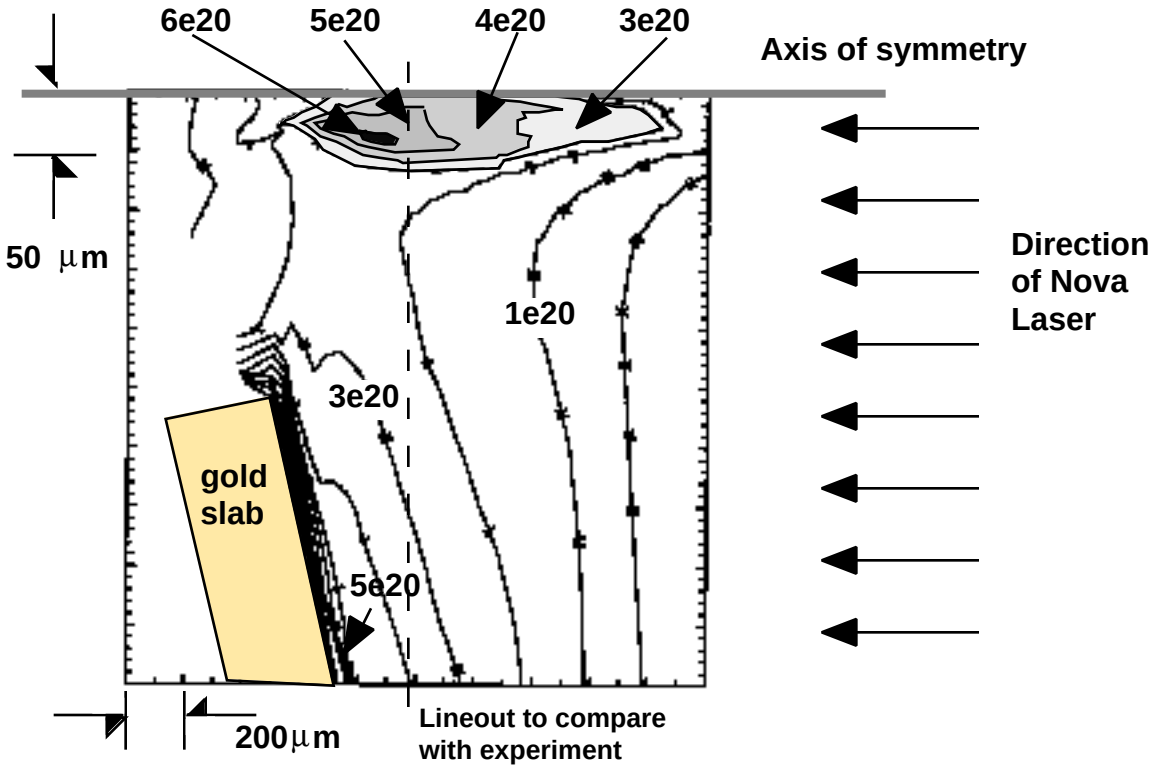

Figure 11 A snapshot of a LASNEX-calculated 2-D n_e profile, using the single-fluid approximation, at a time of 150 ps after the end of a 1-ns-long, temporally squared optical laser pulse, which corresponds to the peak of the x-ray laser pulse that serves as the gate for our imaging setup used in the experiment. This geometry simulates the lower half slab of the experimental configuration shown in Fig. 7. The dashed line represents the position where we took a lineout to compare with the experiment and is shown as the dash-dotted line in Fig. 10.

kind of modeling in dealing with plasmas at this collisionality regime. We are currently working on a 2-D multi-specie fluid code [46,47,48] to serve as our numerical model for this set of colliding plasma experiments.

4. Development of Enhanced-coherence X-ray Lasers

In collisionally excited x-ray lasers, laser gain is sensitively dependent on plasma conditions. When line-focused optical laser incident on a uniformly coated solid target, the laser-driven plasma expands in two dimensions with large electron density gradients both parallel and perpendicular to the target surface. The position of the gain region continuously shifts to the location of optimum plasma conditions. Laser photons propagate in a highly refractive medium which cause typical laser divergence of order 10 mrad by 16-20 mrad [49].

The concept of adaptive spatial filtering of an x-ray laser uses geometric shaping to control the laser aperture. This could be in a conical or bowtie shape. In the unsaturated regime, rays that traverse the longest gain regions have the possibility of attaining the most gain-lengths (GL) and highest output intensities. The neck of a bowtie laser acts as a narrow spatial filter where the high GL rays must pass through. These high GL rays have strong correlation between their angle of tilt and their transverse positions. Rays that travel outside of the bowtie neck achieve lower GL and are attenuated by surrounding materials.

In the saturated regime, bowtie x-ray lasers actually increase the coherent power by causing significant power extraction into only a few modes and by eliminating parasitic modes. In saturation the effective (or loaded) gain depends on the overall intensity pattern in a non-linear and self-consistent way. The maximum gain of a saturated bowtie x-ray laser is located at the neck region where the adaptive spatial filtering occurs. This effective spatial gain distribution maintains the correlation between ray tilt and transverse position at the laser output end that is needed to achieve high coherent power. Thus the energy content of a saturated x-ray laser preferentially flows through the few Fresnel zones defined by the neck of the bowtie. In a non-refractive and uniform-gain medium, with all the energy extracted, the output intensity of a bowtie x-ray laser would be weaker than that of a stripe x-ray laser by the ratio of active gain volumes between the two geometries. However the coherent power of a bowtie x-ray laser would be much stronger than that of a stripe x-ray laser.

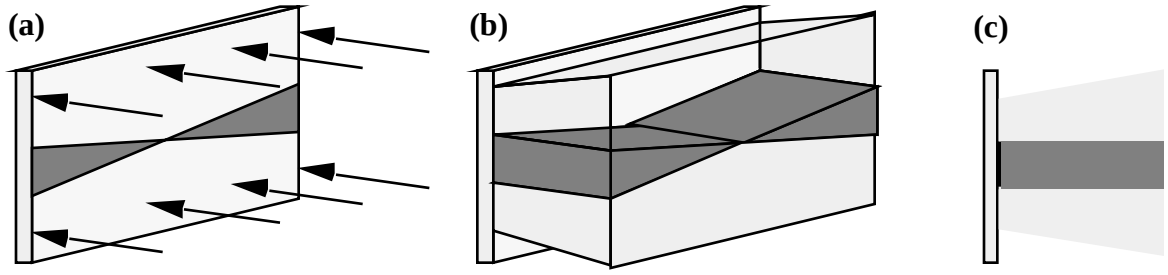

Figure 12. (a) Incoming optical laser overfills a bowtie-shaped x-ray laser (dark region) deposited on similar-Z substrate (light region) and produces a more one-dimensional hydrodynamic expansion of the x-ray laser plasma (b, c) which maintains the geometric shape of the bowtie laser during expansion.

A key issue in the performance of bowtie x-ray lasers is our ability to maintain the bowtie shape during the plasma expansion. We have several design options for a more hydrodynamically stable x-ray laser. One way to fabricate a bowtie x-ray laser is to deposit a bowtie-shaped thin film coating on a thick substrate. The substrate is made of similar-Z material such that the substrate plasma provides a hydrodynamic tamper to the x-ray laser plasma and maintains the bowtie shape during the lasing period. Figure 12(a) shows the incoming optical laser overfilling the bowtie x-ray laser and producing a one-dimensional (1-D) blow-off near the x-ray laser plasma as shown in Figs 12(b) and 12(c). Such one-dimensionally expanding plasmas should also provide a flatter transverse n_e profile in the lasing region and reduce the transverse laser divergence.

We have performed numerical simulations and a series of Nova experiments to characterize the stripe x-ray laser as the first step in demonstrating our ability to control the x-ray laser shape during plasma expansion. [50] We performed a series of 2-D LASNEX calculations simulating the line-focused slab and stripe x-ray laser geometries. We found a similar-Z hydrodynamic tamper, such as copper on germanium, can effectively control the x-ray laser plasma expansion to 1-D. Figures 13 and 14 show the comparisons of tamped and untamped germanium x-ray laser targets. Pin-hole camera images contrasting the stripe and slab emission features qualitatively confirmed our LASNEX results.

At or near saturation the stripe x-ray laser intensities are comparable to a line-focused slab x-ray laser. The comparable laser intensities indicate no significant differences in gains and refractive ray propagation between the two laser configurations. The bowtie x-ray laser intensities were factors of 10 – 15 lower than the intensities for saturated stripe and slab x-ray lasers. This intensity difference is likely due to less gain medium of the bowtie configuration. However, the coherent power of a saturated bowtie should be stronger than for the other laser configurations. X-ray emission spectra in the 8 – 11-Å range of the foil, slab, stripe, and bowtie targets found contributions dominated by

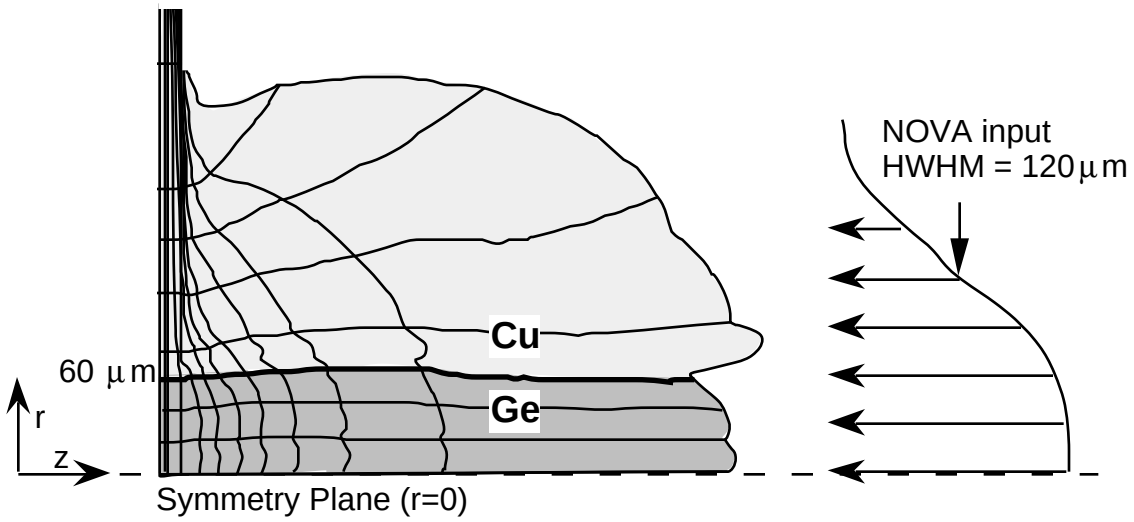

Figure 13. LASNEX-calculated 2-D plasma expansion due to 240-μm line-focused (FWHM) Nova laser incident on a 60-μm germanium stripe coated on solid copper substrate, at 500 ps into the Nova pulse. The copper acts as a tamper to confine the germanium x-ray laser plasma, controlling the source size and reduce density gradient in the *r*-direction.

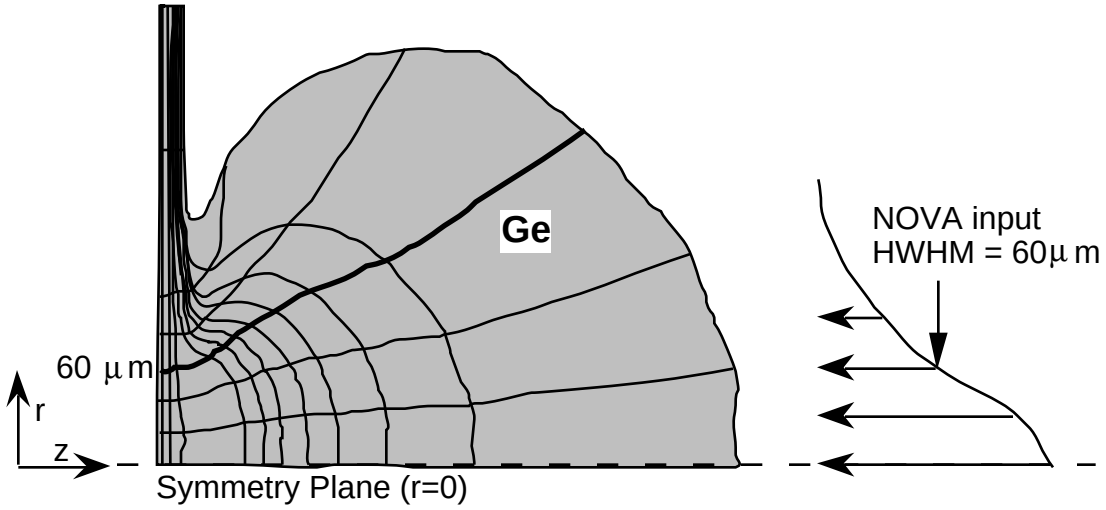

Figure 14. LASNEX-calculated 2-D plasma expansion due to 120-μm line-focused (FWHM) Nova laser incident on uniformly coated, or untamped, germanium slab target, at 500 ps into the Nova pulse, showing significant expansion in the *r*-direction. This expansion results in large density gradient and greater refraction.

neonlike germanium lines, and a forest of copper lines ranging from nitrogen- to neonlike. Intensities of copper and germanium emissions are in agreement with the types of x-ray lasers fielded. The comparable temporal histories of the identified neonlike germanium 3d and 3s $\rightarrow$ 2p emission lines indicate comparable ionization histories between the slab and stripe x-ray lasers.

Depending on future Nova shot availability on the development of enhanced-coherence x-ray lasers, we have plans to further enhance the bowtie output by varying Nova pulse shapes, using new x-ray laser target designs, and using multiple-staged oscillator-amplifier configurations. We are also planning further characterization of stripe and bowtie x-ray lasers, such as measurements of small signal gains, plasma expansion characteristics, and coherence. A bright, coherent x-ray laser source has potential applications in imaging rapidly evolving high density plasmas, and a short-wavelength bowtie x-ray laser, such as a nickellike tantalum x-ray laser with laser wavelength of 44.8 Å, has significant potential in biological imaging and holography applications.

5. Other Potential Applications of Soft X-ray Laser Interferometry

Interferometry has found numerous applications in science and industry. These applications include extremely high resolution measurements of surface properties of media, measurements of absolute indexes of refraction, acquiring the surface figure of optical elements under manufacture, performing ultrahigh resolution spectroscopy, and mapping convective matter flow in liquids, gases and plasmas. The fundamental limiting factor in the accuracy of interferometry has been the wavelength of the system. Interferometric measurement resolution is at least linear in the wavelength. So, for example, an order of magnitude reduction in wavelength with equivalent throughput translates into an order of magnitude or more improvement in the precision of measurements.

Conventional interferometers operate at UV and optical wavelengths (2500 - 7000 Å) or longer. To dramatically reduce the wavelength and move into a regime of precision unexplored in interferometry, the soft x-ray interferometer that we have development under this LDRD project is a high throughput instrument capable of operating over a range of soft x-ray wavelengths (30 - 400 Å). This development required precision engineering at the atomic level in order to allow the fabrication of high efficiency multilayer mirrors and beam splitters inherent in the design. The interferometer we used to obtain two-dimensional density maps of large, dense plasma flows described in Sec. 3 and 4 of this report is a low bandpass, high throughput interferometer optimized at 155 Å, well-suited for a Nova-driven x-ray laser source at LLNL. By using our interferometer instead of a 2500 Å commercial device, we obtained more than a **two order** of magnitude improvement in accuracy due to reduced light refraction in the plasma and more than a **three order** of magnitude enhancement in signal strength because of reduced absorption. This is a unique technology that will enable critical measurements and unprecedented precision in high

intensity laser research associated with the inertial confinement fusion program. These same advantages can be immediately transferred to industry in a variety of applications.

Many companies manufacture commercial optical and infrared interferometers: Zygo (Middlefield, CT), WYKO (Tucson, AZ), and Perkin Elmer (Norwalk, CT) are three examples. Fewer companies manufacture UV interferometers; Zygo sells a high throughput imaging unit operating at 2480 Å (System 248PM1). There are no commercial interferometers available at wavelengths shorter than 2480 Å. Our product operates in a wavelength regime heretofore completely unexplored by interferometers. Table 1 compares the specifications of our soft x-ray interferometer with the current state-of-the-art instrument commercially available.

The soft x-ray interferometer offers a dramatic increase in accuracy in all aspects of precision metrology compared with current state of the art interferometers. It also opens new avenues for the

	Soft X-ray Interferometer	**Commercial interferometer**
Operating Wavelength	155 Å (30 - 400 avail.)	2480 Å (longer avail.)
Optics	Multilayer	Dielectric
Spatial Resolution Planar	0.1 micron	0.2 micron
Spatial Resolution Vertical (Depth)	5 Å (λ/30)	60 Å (λ/40)
Tested Resistance to Refraction*	250	1
Tested Signal Gain Due to Decreased Absorption*	4000	1
Cost†	$10K - 50K	$640K

Table: Comparisons of the specifications of our soft x-ray interferometer with the current state-of-the-art instrument commercially available.

* Expressed as a ratio normalized to 1.0 for the state of the art commercial product; larger is better

† Cost for the soft x-ray interferometer is for multilayer optics and hardware only; cost of the 2480 Å system is for a turnkey unit including source and data acquisition equipment

examination of material properties. These improvements are made possible by the much shorter operating wavelength of our interferometer compared with existing interferometric systems. The shortest wavelength interferometer commercially available operates in the UV at 2480 Å. Our present high efficiency system is optimized for 155 Å, a factor of 15 smaller. We can build high throughput interferometers that operate as short as 30 Å or as long as 400 Å. This wavelength regime has not been exploited by commercial optics manufacturers due to difficulty in fabricating efficient multilayer optics at these wavelengths.

In applications involving mapping and range finding, the soft x-ray interferometer provides more than an order of magnitude improvement in resolution compared to the current state of the art. Comparing specifically with the 2480 Å commercial model, we obtain a factor of 15 better spatial resolution. We are thus able to detect morphological defects or imperfections an order of magnitude smaller than is now possible. This has an immediate effect on the fabrication of optical components. The fundamental limitation in optics manufacture is the resolution with which components can presently be characterized. Our product, with a factor of 15 better resolution than current units, can dramatically improve the fabrication of optical components.

Optical elements cannot now be characterized in the sub-UV wavelength regime. The soft x-ray interferometer extends characterization measurements down to 30 Å. This is especially important for measuring the figure and phase of multilayer x-ray optics such as those being developed for use in the next generation of x-ray lithography systems. Present interferometers cannot characterize multilayer x-ray optics in the wavelength range at which the components are intended to operate. The surface figure of multilayers is presently measured at wavelengths 15 to 100 times the wavelength for which the multilayer was designed. Not only is resolution lost in the surface figure (as described above), but phase shifts introduced by the series of layer pairs that make up the element are undetectable. For multilayer x-ray optics, our soft x-ray interferometer permits the measurement of both high resolution surface figure and phase information.

The soft x-ray interferometer opens up a new wavelength range in the study of material properties that competing interferometric devices cannot access. Optical properties of solid state materials can be examined in a regime where the light has sufficient energy to probe electronic energy bands, molecular bonding, and other effects.

Interferometry can be used to accurately measure the index of refraction of materials. Shorter wavelengths permit remarkably better signal properties in the characterization of high density plasmas. Compared to the best available commercial interferometer, the soft x-ray interferometer

provides a more than two order of magnitude enhancement in resolution due to reduced refraction in a plasma and a more than three order of magnitude increase in signal due to decreased absorption. This permits measurements of plasmas at higher densities, larger volumes, and with more severe gradients than is possible with conventional instruments.

One potential application of soft x-ray interferometry is ultrahigh precision Fourier transform spectroscopy in a heretofore unreachable regime. An interferometer can be used to directly measure the temporal autocorrelation function of the input beam. Fourier inversion of the measurement reveals the input spectrum. Commercial Fourier transform spectrometers are available in the optical and longer wavelength ranges. Operating our interferometer at soft x-ray wavelength opens up the possibility of performing high resolution absorption (or emission) spectroscopy. It also would allow the interferometer to function in a scanning mode which would provide still higher spatial resolution.

Applications of our product are not restricted to national laboratories. Our product can be used with any source of x rays possessing a longitudinal coherence of approximately one micron (or more). An x-ray line source such as a commercially available rotating anode type, a high order harmonic converter on a laser, a laser produced plasma, or a synchrotron beamline can all be used. A soft x-ray laser can and has been used. We note that alignment of the interferometer can be easily accomplished with a white light source.

6. Summary and Future Directions

Our targeted deliverable at the end of this three-year project is to deliver a high-resolution, high-throughput plasma imaging diagnostic that is capable of studying plasmas in a high energy density physics regime that was previously inaccessible. We have successfully achieved our primary objective in the demonstration of the soft x-ray laser interferometer. We obtained data not possible by other means: the soft x-ray interferometer provided a two order of magnitude improvement in accuracy due to reduced light refraction in the plasma and more than a three order of magnitude enhancement in signal strength because of reduced absorption. The soft x-ray interferometer is an enabling technology in the diagnosis of large, high density plasmas and will have important impact for both the ICF and weapon physics communities, for analyzing current experiments on Nova and, in the future, on the National Ignition Facility.

The successful demonstration of the soft x-ray interferometer on the Nova 2-beam facility illustrates the important role short wavelength interferometry can play in diagnosing laser-produced plasmas. Using the soft x-ray interferometry technique, we have already studied a variety of laser-produced plasmas. The results of these experiments have received international recognition and have been published, or will be published shortly, over 10 refereed journal papers. We have studied the multilayer damage threshold on the Nova 10-beam facility and are planning a series of experiments to study the dynamics of ICF-relevant plasmas, such as capsules and hohlraums.

Detailed comparisons of two-dimensional electron density profiles obtained from soft x-ray interferograms and profiles obtained from radiation hydrodynamics codes, such as LASNEX, will allow us to validate and benchmark complex numerical models used to study the physics of laser-plasma interactions. The ultimate motivation of the development of soft x-ray interferometry technique is to provide a mechanism to probe the deficiencies of our numerical models in areas such as laser deposition by both resonance and inverse bremsstrahlung absorption, flux-limited heat conduction, hydrodynamics, and non-local thermodynamics equilibrium atomic kinetics.

Soft x-ray interferometer has potential applications in areas other than probing laboratory plasmas. The development of an interferometer capable of operating in the wavelength range from 30 - 400 Å is a technical innovation that represents a more than ten-fold enhancement in precision over present generation interferometers. This soft x-ray interferometer opens the door to performing interferometric measurements in a wavelength regime never before accessed by a commercial product. For example, it can be used to characterize the figure and phase properties of multilayer mirrors near their intended operating wavelength. This is important because multilayer mirrors introduce a phase shift which is sensitive not only to the surface figure but also the multilayer structure. The soft x-ray interferometer can also be used to measure spectral lineshapes with resolutions far exceeding those currently possible.

Acknowledgments

The authors are just the principle and co-investigators of this project. There were many contributors over the course of the three-year period when this project was funded by LDRD that resulted in the successes of this project. We would especially like to acknowledge the contributions of Troy Barbee, Jr., who led the development of the multilayer optics; Dino Ciarlo, who fabricated most of the multilayer optics. Peter Celliers and Franz Weber were instrumental in the development of the interferometer and performed most of the alignments of the optical components. Jim Trebes is leading the implementation of the soft x-ray laser interferometer on the 10-beam. Rich London

provided much of the numerical modeling expertise and along with Chris Decker performed the modeling of the hohlraum probing experiment. Hedley Louis and Tony Demeris made most of the shaped and multi-components x-ray laser targets while Gary Stone provided hohlraum and colliding plasma targets. X-ray laser foils and much of the filters were made by Luxel Corp., led by Forbes Powell. Sharon Alvarez is primarily responsible for x-ray laser target assembly and alignment, and also multilayer reflectivity calibration, support by Andy Nikitan and Joe Smith. We would also like to acknowledge the support of all the Nova engineers and technicians, especially the 2-beam technicians, led by Jeff Cardinal, and including Jeff Robinson and Dennis Cocherell. Jim Cox made many of the components for the interferometer. Finally, we would like to acknowledge the helpful discussions and support of physicists at A-, X-, and Y-Divisions, including Joe Nilsen, Jeff Koch, Dick Lee, Mordy Rosen, Sam Dalhed, Howard Scott, Brian MacGowan, Peter Rambo, and Dennis Matthews.

References

1. D. Matthews *et al*., *Phys. Rev. Lett.* **54**, 110–113 (1985).
2. See papers in *Proc. of the Applications of X-ray Lasers Workshop*, edited by R. A. London, D. L. Matthews, and S. Suckewer, Report CONF-9206170 Lawrence Livermore National Laboratory (January 1992).
3. E. Spiller, Soft X-ray Optics (SPIE, Bellingham, WA, 1994).
4. R. Cauble *et al*., *Phys. Rev. Lett.* **74**, 3816 – 3819 (1995)
5. D. Ress *et al*., *Science* **265**, 514 (1994).
6. M. Rosen *et al*., *Phys. Rev. Lett.* **54**, 106–109 (1985).
7. G. Charatis *et al*., *Journal De Physique* **C6**, 89-98 (1986).
8. M. K. Prasad *et al*., *Phys. Fluids B* **4**, 1569 (1992).
9. D. T. Attwood *et al*., *Phys. Rev. Lett.* **40**, 184 (1978).
10. P. E. Young, *Phys. Fluids B* **3**, 2331-2336 (1991).
11. S. Wilks *et al*., *Phys. Rev. Lett.* **73**, 2994-2997 (1994).
12. C. W. Allen, *Astrophysical Quantities*, p. 100 (Oxford University Press, New York, 1963).
13. J. Koch *et al*., *Phys. Rev. Lett.*, **68**, 3291 (1992).
14. T. W. Barbee Jr. *et al*., *Appl. Opt.* **32**, 4852-4854 (1993).
15. D. G. Stearns *et al*., *J. Vac. Sci. Technol. A, Vac. Surf. Films* **9**, 2662-2669 (1991).
16. L. B. Da Silva *et al*., *Phys. Rev. Lett.* **74**, 3991 – 3994 (1995)
17. P. Celliers *et al*., *Optics Letter* **20**, 1907 – 1909, (1995).
18. A. S. Wan *et al*., to be published in *J. Opt. Society of America B: Optical Physics*
19. L. B. Da Silva *et al*., to be published in *IEEE, Transactions in Plasma Science* (1996).
20. A. S. Wan *et al*., to be submitted to Phys. *Rev. Lett.*
21. G. B. Zimmerman and W. L. Kruer, *Com. Plasma Phys. and Cont. Fusion*, **2**, 51 (1975).
22. M. K. Prasad *et al*., *Phys. Fluids B* **4**, 1569 (1992).
23. D. Ress *et al*., *Phys. of Fluids B* **2**, 2448 (1990); E. F. Gabl *et al.*, *Phys. Fluids B* **2**, 2437 (1990).
24. A. R. Bell, R. G. Evans, D. J. Nicholas, *Phys. Rev. Lett.* **46**, 243 (1981).
25. J. H. Rogers *et al*., *Phys. Fluids B* **1**, 741 (1989).
26. W. C. Mead *et al*., *Phys. Fluids* **26**, 2316 (1983).
27. M. Rosen *et al*., *Phys. Rev. Lett.* **54**, 106–109 (1985).
28. G. Charatis *et al*., *J. de Physique* **C6**, 89-98 (1986).
29. M. Rosen *et al*., *Bull. Am. Phys. Soc.*, **27**, 989 (1982); W. B. Fechner et al., *Phys. Fluids* **27**, 1552 (1984).
30. S. W. Haan, *et al*., *Phys. Plasmas* **2**, 2480–2487 (1995).

31. G. Charatis *et al.*, *J. Phys. Coll. C* **47**, 6 (1986); T. Boehly *et al.*, *Appl. Phys. B* **50**, 165 (1990); and P. Glas, M. Schnurer, *Laser Part. Beams* **9**, 501 (1992).
32. J. E. Balmer, R. Wever, P. F. Cunningham, P. Ladrach, *Laser Part. Beams* **8**, 327 (1990).
33. R. W. Clark, *et al.*, "Soft X-ray Lasers and Applications," SPIE Proceeding **2520** 340 –346 (1995).
34. L. V. Powers *et al.*, *Phys. Plasmas* **2**, 2473 – 2479 (1995); L. V. Powers *et al.*, *Phys. Rev. Lett.* **74**, 2957 – 2960 (1995).
35. D. H. Kalantar *et al.*, *Phys. Plasmas* **2**, 3161 – 3168 (1995).
36. J. Lindl, *Phys. Plasmas* **2**, 3933 (1995).
37. W. J. Krauser *et al.*, to be published in *Phys. Plasmas*.
38. R. S. Bosch *et al.*, *Phys. Fluids B* **4**, 979 – 987 (1992).
39. S. M. Pollaine *et al.*, *Phys. Fluids B* **4**, 989 – 991 (1992).
40. R. L. Berger *et al.*, *Phys. Fluids B* **3**, 3 (1991).
41. C. A. Back *et al.*, *Rev. Sci. Instr.* **66**, 764 (1995).
42. O. Larroche, *Phys. Fluids B* **5**, 2816 (1993).
43. M. D. Wilke *et al.*, to be published in "Applications of Laser Plasma Radiation II," SPIE Proceeding **2523** (1995).
44. O. Rancu *et al.*, Phys. Rev. Lett. **75** 3854-3857 (1995).
45. T. S. Perry, R. I. Klein, private communications.
46. P. W. Rambo, private communications.
47. P. W. Rambo, J. Denavit, *Phys. Plasmas* **1**, 4050–4060 (1994).
48. P. W. Rambo, R. J. Procassini, *Phys. Plasmas* **2**, 3130–3145 (1995).
49. J. E. Trebes *et al.*, Phys. Rev. Lett. **68**, 588 (1992).
50. A. S. Wan *et al.*, *Optical Engineering*, **33** (7), 2434 – 2441 (1994).

Appendix

Journal and conference papers and presentations relevant to the LDRD-funded project: "X-ray Laser Propagation and Coherence: Diagnosing Fast-evolving, High-density Laser Plasmas Using X-ray Lasers."

I. Research and development of soft x-ray interferometer:

I.1 journal papers

XUV Interferometry at 155Å Using Multilayer Optics
L. B. Da Silva, T. W. Barbee, Jr., R. Cauble, P. Celliers, D. Ciarlo, J. C. Moreno, S. Mrowka, J. E. Trebes, A. S. Wan, F. Weber
Applied Optics, **34**, 378 (1995).

Electron Density Measurements of High Density Plasmas using Soft X-ray Laser Interferometry
L. B. Da Silva, T. W. Barbee, Jr., R. Cauble, P. Celliers, D. Ciarlo, S. Libby, R. A. London, D. Matthews, J. C. Moreno, D. Ress, J. E. Trebes, A. S. Wan, F. Weber
Physics Review Letters, **74**, 3991 – 3994 (1995).

High Density Plasma Diagnostics Utilizing a Neonlike Yttrium X-ray Laser
R. Cauble, L. B. Da Silva, T. W. Barbee, Jr., P. Celliers, S. Libby, J. C. Moreno, D. Ress, J. Trebes, A. S. Wan, F. Weber
Journal of Quantum Spectroscopy and Radiative Transfer, **54**(12), 97 – 103 (1995).

X-ray Lasers for High Density Plasma Diagnostics
L. B. Da Silva, T. W. Barbee, Jr., R. C. Cauble, P. Celliers, J. Harder, H. R. Lee, R. A. London, D. L. Matthews, S. Mrowka, J. C. Moreno, D. Ress, J. E. Trebes, A. Wan, F. Weber
Review of Scientific Instruments, **66**, 574 – 578 (1995).

X-ray Lasers Shrink in Size and Wavelength
E. Fill
Opto & Laser Europe, **18**, 30 – 32 (March 1995).

X-ray Lasers and High-density Plasma
L. B. Da Silva, R. C. Cauble, S. B. Libby
Energy & Technology Review, published by the Lawrence Livermore National Laboratory as LLNL Report Number UCRL-52000-95-3, 9 – 19 (March 1995).

I.2 Conference papers and presentations

Electron Density Measurements of High Density Plasmas using Soft X-ray Laser Interferometry (invited talk)
L. B. Da Silva, T. W. Barbee, Jr., R. Cauble, P. Celliers, D. Ciarlo, S. Libby, R. A. London, D. Matthews, J. C. Moreno, D. Ress, J. E. Trebes, A. S. Wan, F. Weber
5th International Colloquium on X-ray Lasers, Lund
Sweden, June 1996.

X-ray Laser Interferometry: A New Tool for AGEX
A. S. Wan, J. C. Moreno, S. B. Libby, R. Cauble, T. W. Barbee, Jr., P. Celliers, L. B. Da Silva, R. A. London, J. E. Trebes, and F. Weber

Proceeding of the 10th Nuclear Explosives Design Physics Conference, Los Alamos (1995).

The X-ray Laser as a Tool for Imaging Plasmas (invited talk)
S. B. Libby, L. B. Da Silva, T. W. Barbee, Jr., R. Cauble, P. Celliers, R. A. London,
D. L. Matthews, S. Mrowka, J. C. Moreno, J. E. Trebes, D. Ress, A. S. Wan, F. Weber
Proceeding of the 12th Int'l. Conf. on Laser Interaction and Related Plasma Phenomena
Osaka, Japan, April 1995.

X-ray Laser Interferometry (invited talk)
L. Da Silva, T. W. Barbee, Jr., R. Cauble, P. Celliers, S. Libby, J. C. Moreno, J. Trebes,
A. S. Wan and F. Weber
International Workshop on X-ray Lasers and Optics, Mianyang, China (1995).

Development of XUV-interferometry (155 Å) Using a Soft X-ray Laser (invited talk)
L. B. Da Silva, T. W. Barbee, Jr., R. Cauble, P. Celliers, D. Ciarlo, S. Libby, R. A. London,
D. L. Matthews, S. Mrowka, J. C. Moreno, J. E. Trebes, A. S. Wan, F. Weber
"Soft X-ray Lasers and Applications," SPIE Proceeding Series **2520**, pp 288 – 296
J. Rocca and P. L. Hagelstein, editors
SPIE Annual Conference 1995, 9-14 July, 1995, San Diego.

The X-ray Laser as a Tool for Imaging Plasmas (invited talk)
S. Libby, L. Da Silva, T.W. Barbee, Jr, R. Cauble, P. Celliers, H.R. Lee, R. London, D.L.
Matthews, S. Mrowka, J.C. Moreno, D. Ress, J.E. Trebes, A. Wan, F. Weber, B. Van Wonterghem
7th IEEE Lasers and Electro-optics Society Meeting, Boston (1994).

High Density Plasma Diagnostics using X-ray Lasers (invited talk)
R. Cauble L. B. Da Silva, T.W. Barbee, Jr., S. Libby, J. C. Moreno, D. Ress, J. Trebes,
A. S. Wan, F. Weber
6th International Workshop on the Radiative Properties of Hot Dense Matter, Sarasota, FL (1994).

X-ray Laser Interferometry for Probing High Density Plasmas
L.B. Da Silva, T.W. Barbee, Jr, R. Cauble, P. Celliers, H.R. Lee, D.L. Matthews, S. Mrowka,
J.C. Moreno, D. Ress, J.E. Trebes, A. Wan, and F. Weber,
Bulletin of the American Physical Society, **39**, 1723 (1994).

X-Ray Laser For Imaging and Plasma Diagnostics (invited talk)
L. B. Da Silva, T. W. Barbee, Jr., R. C. Cauble, P. Celliers, J. Harder, S. B. Libby, H. R. Lee, R.
A. London, D. L. Matthews, S. Mrowka, J. C. Moreno, D. Ress, J. E. Trebes, A. S. Wan, F. Weber
"X-ray Laser 1994," AIP Conference Proceeding **332**, pp 553 – 558,
Proceed. of the 4th International Colloquium on X-Ray Lasers, D. Matthews, D. C. Eder, editors
American Institute of Physics Press, Woodbury, NY, 1994.

Multilayer Optics for X-Ray Laser Instrument (invited talk)
T. W. Barbee, Jr.
4th International Colloquium on X-Ray Lasers
Williamsburg, VA, May 16–20, 1994.

Recent Progress in X-ray Laser Research at LLNL (invited talk)
J. Koch, T. Barbee, P. Batson, L. Da Silva, R. Cauble, P. Celliers, L. Klein, H. Lee, R. Lee,
S. Libby, R. London, B. MacGowan, D. Matthews, J. Moreno, S. Mrowka, J. Nilsen, D. Ress,
J. Scofield, J. Trebes, J. Underwood, B. Van Wonterghem, A. Wan, and F. Weber
Int'l. Conf. of Short Wavelength Radiation and Applications, Zvenigorod, Russia (August, 1994).

Recent Developments in X-ray Lasers and their Applications (invited seminar)
L. B. Da Silva, T. Barbee, R. Cauble, D. Eder, J. Koch, R. London, S. Mrowka, B. MacGowan, D. Matthews, S. Maxon, D. Ress, B. Van Wonterghem, J. Trebes, P. Amendt, R. Ratkowsky, A. Osterheld, A. Wan, R. Balhorn, T. Donnelly, R. Falcone, E. Anderson, and J. Underwood
seminar presented at Washington State University, Pullman (November, 1993).

Development of Compact X-ray Lasers and their Applications (invited talk)
L. B. Da Silva, J. Koch, B. MacGowan, D. Matthews, S. Mrowka, D. Ress, J. Trebes, B. Van Wonterghem, R. Cauble, R. London, D. Eder, P. Amendt, R. Ratowsky, J. Moreno, J. Nilsen, A. Osterheld, A. Wan, R. Balhorn, and T. Barbee
1993 Symposium on Coherent Radiation Sources, Berkeley (1993).

II. Application of soft x-ray interferometer:

II.1 journal papers

Electron Density Measurement of a Colliding Plasma Using Soft X-ray Laser Interferometry
A. S. Wan, T. W. Barbee, Jr., R. Cauble, P. Celliers, L. B. Da Silva, J. C. Moreno, P. W. Rambo, G. F. Stone, J. E. Trebes, and F. Weber
in preparation, to be submitted to *Physics Review Letters.*

Measurement of Local Gain and Electron Density in an Yttrium X-ray Laser Amplifier
R. Cauble, L. B. Da Silva, T. W. Barbee, Jr., P. Celliers, R. A. London, J. C. Moreno, A. S. Wan, and F. Weber
in preparation, to be submitted to *Physics Review Letters.*

Application of X-ray Laser to Probe High-density Plasmas
L. B. Da Silva, T. W. Barbee, Jr., R. Cauble, P. Celliers, D. H. Kalantar, M. H. Key, S. Libby, D. L. Matthews, J. C. Moreno, J. E. Trebes, A. S. Wan, F. Weber
in preparation, to be submitted to *Physics of Plasmas.*

Two-dimensional Interferogram of an Exploding Selenium Foil using a Soft X-ray Laser Interferometer
L. B. Da Silva, T. W. Barbee, Jr., R. Cauble, P. Celliers, D. Ciarlo, S. Libby, R. A. London, D. L. Matthews, J. C. Moreno, D. Ress, J. E. Trebes, A. S. Wan, F. Weber
to be published in *IEEE, Transactions in Plasma Science* (1996);
UCRL-JC-120706.

Application of X-Ray Laser Interferometry to Study High-density Laser-produced Plasmas
A. S. Wan, L. B. Da Silva, T. W. Barbee, Jr., R. Cauble, P. Celliers, S. B. Libby, R. A. London, J. C. Moreno, J. E. Trebes, F. Weber
to be published in *Journal of Optical Society of America B: Optical Physics* (1996);
UCRL-JC-120592.

Fringe Formation and Coherence of a Soft X-ray Laser Beam Illuminating a Mach-Zehnder Interferometer
P. Celliers, F. Weber, L. B. Da Silva, T. W. Barbee, Jr., R. C. Cauble, A. S. Wan, J. C. Moreno
Optics Letter **20**, 1907 – 1909, (1995).

Micron-scale Resolution Radiography of Laser Accelerated Foils using X-Ray Lasers
R. Cauble, L. B. Da Silva, T. W. Barbee, Jr., P. Celliers, J. C. Moreno, S. Mrowka, T. S. Perry, and A. S. Wan

Physics Review Letters, **74**, 3816 – 3819 (1995).

II.2 Conference papers and presentations

Application of Soft X-ray Laser Interferometry to Study Large-scale-length, High-density Plasmas (invited talk)
A. S. Wan, T. W. Barbee, Jr., R. Cauble, P. Celliers, L. B. Da Silva, J. C. Moreno, R. A. London, P. W. Rambo, G. F. Stone, J. E. Trebes, and F. Weber
5th International Colloquium on X-ray Lasers, Lund
Sweden, June 1996.

Design and Analysis of X-ray Laser Probing Experiment of Hohlraums (invited talk)
C. Decker, R. A. London, L. Powers, J. A. Harte, J. E. Trebes, D. B. Ress, L. B. Da Silva, M. K. Prasad, A. S. Wan, R. Cauble, P. Celliers, F. Weber
5th International Colloquium on X-ray Lasers, Lund
Sweden, June 1996.

Electron Density Measurement of a Colliding Plasma using Soft X-ray Laser Interferometry
A. S. Wan, T. W. Barbee, R. Cauble, P. Celliers, L. B. Da Silva, J. C. Moreno, P. W. Rambo, G. F. Stone, J. E. Trebes and F. Weber
24th European Conference on Laser Interactions with Matter, Madrid (1996).

Measurement of Local Gain and Electron Density in an Yttrium X-ray Laser Amplifier
R. Cauble, T. W. Barbee, Jr., L. B. Da Silva, P. Celliers, R. A. London, J. C. Moreno, J. E. Trebes, A. S. Wan, and F. Weber
24th European Conference on Laser Interactions with Matter, Madrid (1996).

Soft X-ray Probing of Dense Plasmas (invited talk)
F. Weber, L. B. Da Silva, T. W. Barbee, Jr., R. Cauble, P. Celliers, J. C. Moreno, J. Trebes, A. S. Wan
Lasers '95, Charleston, SC (1995).

Application of X-ray Laser to Probe High-density Plasmas (invited talk)
L. B. Da Silva, T. W. Barbee, Jr., R. Cauble, P. Celliers, D. H. Kalantar, M. H. Key, S. Libby, D. L. Matthews, J. C. Moreno, J. E. Trebes, A. S. Wan, F. Weber
37th Annual Meeting of the Div. of Plasma Physics of the American Physical Society.

Application of X-ray Laser Interferometry to Study High-density, Laser-produced Plasmas
A. S. Wan, L. B. Da Silva, T. Barbee, Jr., R. Cauble, P. Celliers, C. Decker, S. Libby, R. A. London, J. C. Moreno, J. E. Trebes, and F. Weber
Bulletin of the American Physical Society, **40**, 1831 (1995).

X-ray Laser Interferometry of Exploding X-ray Laser Foils
R. Cauble, T. W. Barbee, Jr., P. Celliers, L. B. Da Silva, C. Decker, R. A. London, J. C. Moreno, J. E. Trebes, A. S. Wan, and F. Weber
Bulletin of the American Physical Society, **40**, 1831 (1995).

Simulations of X-ray Laser Probing of Hohlraums
R. London, C. Decker, L. Powers, J. Harte, J. E. Trebes, R. Cauble, A. S. Wan, L. B. Da Silva
Bulletin of the American Physical Society, **40**, 1831 (1995).

X-ray Laser Probing of Hohlraums
J. E. Trebes, T. W. Barbee Jr, R. Cauble, P. Celliers, L. Da Silva, C. Decker, R. London,

J. C. Moreno, D. Ress, A. S. Wan and F. Weber
Bulletin of the American Physical Society, **40**, 1831 (1995).

Application of Soft X-ray Lasers for Plasma Diagnostics (invited talk)
P. Celliers, T. W. Barbee, Jr., R. Cauble, L. B. Da Silva, J. C. Moreno, D. Ress,
J. E. Trebes, A. S. Wan, F. Weber
Proceeding of the 8th IEEE Lasers and Electro-Optics Society 1995 Annual Meeting,
Oct. 30 - Nov. 2, 1995, San Francisco.

X-ray Lasers and Applications (invited talk)
L. B. Da Silva, T. W. Barbee, Jr, R. Cauble, P. Celliers, S. Libby, J. C. Moreno, J. Trebes,
A. S. Wan and F. Weber
Fourth VUV Conference, Tokyo, Japan (1995).

X-ray Laser Interferometry for Probing High-density Plasmas (invited talk)
A. S. Wan, L. B. Da Silva, T. W. Barbee, Jr., R. Cauble, P. Celliers, S. Libby, R. A. London,
J. C. Moreno, J. E. Trebes, F. Weber
"Soft X-ray Lasers and Applications," SPIE Proceeding Series **2520**, pp 268 – 278,
J. Rocca and P. L. Hagelstein, editors
SPIE Annual Conference 1995, 9-14 July, 1995, San Diego.

Design and Analysis of X-ray Laser Probing Experiments of Laser-Fusion Plasmas
R. A. London, C. Decker, L. Powers, J. A. Harte, J. E. Trebes, D. B. Ress, L. B. Da Silva, M.
K. Prasad, A. S. Wan, R. C. Cauble
SPIE Annual Conference 1995, 9-14 July, 1995, San Diego.

Diagnosing High Density, Fast-evolving Plasmas using X-Ray Lasers
R. Cauble, L. B. Da Silva, T. W. Barbee, Jr., P. Celliers, S. Libby, J. C. Moreno, S. Mrowka,
D. Ress, J. E. Trebes, A. S. Wan, F. Weber
Institute Physics Conference Series No. **140**, pp 117 – 120 (1995)
Proceeding of the Laser Interaction with Matters Conf., Oxford, 19–23 September, 1994;
UCRL-JC-116843.

Applications of X-ray Lasers as Plasma Imaging Diagnostics (invited talk)
P. Celliers, L. Da Silva, T. W. Barbee, Jr, R. Cauble, H. R. Lee, R. London, D. L. Matthews, S.
Mrowka, J. C. Moreno, D. Ress, J.E. Trebes, A. Wan, F. Weber, and B. Van Wonterghem
Society for Optical and Quantum Electronics International Conference on Lasers, Québec (1994).

High Resolution Imaging of Laser-Produced Plasmas Using X-ray Lasers
R. Cauble, L. B. Da Silva, T. W. Barbee, Jr., P. Celliers, S. Mrowka, J. C. Moreno, A. Wan,
and F. Weber
Bulletin of the American Physical Society, **39**, 1723 (1994);
UCRL-JC-117812Abs.

Micron-scale Resolution Radiography of Laser Accelerated and Laser-Exploded Foils using an Yttrium X-ray Laser
R. Cauble, L. B. Da Silva, T.W. Barbee Jr, P. Celliers, J. C. Moreno, S. Mrowka, T. S. Perry,
and A. S. Wan
"X-ray Laser 1994," AIP Conference Proceeding **332**, pp 562 – 565,
Proceed. of the 4th International Colloquium on X-Ray Lasers, D. Matthews, D. C. Eder, editors
American Institute of Physics Press, Woodbury, NY, 1994.

Micron-scale Resolution Radiography of Laser Accelerated Foils using an X-ray Laser

R. Cauble, L. B. Da Silva, T.W. Barbee, Jr., J. C. Moreno, S. Mrowka, A. S. Wan, B. Van Wonterghem
4th International Colloquium on X-ray Lasers, Williamsburg (1994)
UCRL-JC-116842Abs.

Application of X-ray Lasers as Imaging and Plasma Diagnostics
A. S. Wan, L. Da Silva, T. Barbee, R. Cauble, P. Celliers, H. Lee, R. London, D. Matthews, S. Mrowka, J. Moreno, D. Ress, J. Trebes, F. Weber, and B. Van Wonterghem
Conf. on High Field Interactions and Short Wavelength Generation, St. Malo, France (August, 1994).

III. Development of advanced x-ray laser sources

III.1 journal papers

Dynamics of a Multiple-Pulse-Driven X-ray Laser Plasma
A. S. Wan, L. B. Da Silva, J. C. Moreno, R. Cauble, P. Celliers, H. E. Dalhed, J. A. Koch, J. Nilsen
Physics of Plasmas; **3**, 606 – 613 (1996).
UCRL-JC-120030.

Spectroscopy and Gain Dynamics Issues in Inhomogeneous X-ray Laser Plasmas
M. Nantel, J. C. Kieffer, J. Dunn, G. D. Enright, D. M. Villeneuve, J. Dunn, A. S. Wan, R. S. Walling, A. L. Osterheld, H. Scott, O. Peyrusse
Journal of Physics B: Atomic, Molecular , and Optical Physics, **28**, 2765 – 2780 (1995).

Characterization of germanium Stripe X-ray Lasers
A. S. Wan, J. C. Moreno, B. J. MacGowan, S. B. Libby, J. A. Koch, J. Nilsen, A. L. Osterheld, J. H. Scofield, J. E. Trebes, R. S. Walling
Optical Engineering, **33** (7), 2434 – 2441 (1994).

Imaging of Laser-Irradiated Targets at a Wavelength of 33.8 Å Using a Normal-Incident Multilayer Mirror
J. F. Seely, C. M. Brown, G. E. Holland, R. W. Lee, J. C. Moreno, B. J. MacGowan, C. A. Back, L. B. Da Silva, and A. S. Wan
Physics of Plasmas, **1** 6, 1997 – 2002 (1994).

III.2 Conference papers and presentations

Characterization and Modeling of Soft X-ray Lasers (invited talk)
A. S. Wan, R. Cauble, P. Celliers, L. B. Da Silva, S. B. Libby, R. A. London, J. Nilsen, J. C. Moreno, F. Weber
Proceeding of the 8th IEEE Lasers and Electro-Optics Society 1995 Annual Meeting
Oct. 30 - Nov. 2, 1995, San Francisco.

Development of a Short Pulse Neon-like X-ray Laser
J. C. Moreno, R. Cauble, P. Celliers, L. B. Da Silva, J. Nilsen, and A. S. Wan
"Soft X-ray Lasers and Applications," SPIE Proceeding Series **2520**, pp 97 – 104,
J. Rocca and P. L. Hagelstein, editors.
SPIE Annual Conference 1995, 9-14 July, 1995, San Diego.

Impact of Three-dimensional Nonuniformity on the Germanium X-ray Laser Output
A. S. Wan, R. W. Mayle, Y. Kato, A. L. Osterheld
Proceeding of the 12th International Conf. on Laser Interaction and Related Plasma Phenomena
Osaka, Japan, April 1995.

Development of X-Ray Laser Architectural Components (invited talk)
A. S. Wan, L. B. Da Silva, J. C. Moreno, R. W. Mayle, R. C. Cauble, S. B. Libby, J. Nilsen, R. P. Ratowsky, H. A. Scott, B. Van Wonterghem
"X-ray Laser 1994," AIP Conference Proceeding **332**, pp 350 – 358,
Proceed. of the 4th International Colloquium on X-Ray Lasers, D. Matthews, D. C. Eder, editors. American Institute of Physics Press, Woodbury, NY, 1994.

Enhanced Brightness X-Ray Lasers
A. S. Wan, R. C. Cauble, L. B. Da Silva, J. C. Moreno, J. Nilsen
Institute Physics Conference Series No. **140**, 455 – 458 (1995)
Proceeding of the Laser Interaction with Matters Conference, Oxford, 19 – 23 September, 1994
UCRL-JC-116841.

Investigation of Multiple Pulse Irradiation of Slab Targets for Neon-like X-ray Lasers
J. C. Moreno, J. Nilsen, A. S. Wan, R. Cauble, E. Chandler, and L. Da Silva
Bulletin of the American Physical Society, **39**, 1558 (1994).

Enhanced Coherence X-ray Laser Experiments and Simulations
A. S. Wan, S. B. Libby, J. C. Moreno
Proceeding of the 11th International Conf. on Laser Interaction and Related Plasma Phenomena, Monterey, CA, October 1993.

Technical Information Department • **Lawrence Livermore National Laboratory**
University of California • Livermore, California 94551